Brain Pathology ISSN 1015-6305

RESEARCH ARTICLE

MIR-137 Suppresses Growth and Invasion, is Downregulated in Oligodendroglial Tumors and Targets CSE1L

Kay Ka-Wai Li[1]; Ling Yang[1]; Jesse Chung-Sean Pang[1]; Aden Ka-Yin Chan[1]; Liangfu Zhou[2]; Ying Mao[2]; Yin Wang[3]; Kin-Mang Lau[1]; Wai Sang Poon[4]; Zhifeng Shi[2]; Ho-Keung Ng[1]

[1] Department of Anatomical and Cellular Pathology, The Chinese University of Hong Kong, Hong Kong.
[2] Department of Neurosurgery, Huashan Hospital, Fudan University, Shanghai, China.
[3] Department of Neuropathology, Huashan Hospital, Fudan University, Shanghai, China.
[4] Neurosurgery Division, Department of Surgery, The Chinese University of Hong Kong, Hong Kong.

Keywords
cell growth, CSE1L, gliomas, invasion, microRNA.

Corresponding authors:
Ho-Keung Ng, MD, Department of Anatomical and Cellular Pathology, The Chinese University of Hong Kong, Hong Kong (E-mail: *hkng@cuhk.edu.hk*)

Received 31 May 2012
Accepted 10 December 2012
Published Online Article Accepted 17 December 2012

Kay Ka-Wai Li and Ling Yang contributed equally to the work and are co-first authors

doi:10.1111/bpa.12015

Abstract

MicroRNA-137 (miR-137) expression has been reported to be decreased in astrocytic tumors in two expression profiling studies but its role in the pathogenesis of oligodendroglial tumors is still limited. In this study, we demonstrate that miR-137 expression is significantly downregulated in a cohort of 35 oligodendroglial tumors and nine glioma cell lines compared with normal brains. Lower miR-137 expression is associated with shorter progressive-free survival and overall survival. Restoration of miR-137 expression in an oligodendroglial cells TC620, and also glioblastoma cells of U87 and U373 significantly suppressed cell growth, anchorage-independent growth, as well as invasion. Demethylation and deacetylation treatments resulted in upregulation of miR-137 expression in TC620 cells. *In silico* analysis showed that CSE1 chromosome segregation 1-like (yeast) (CSE1L) is a potential target gene of miR-137. Luciferase reporter assay demonstrated that miR-137 negatively regulates CSE1L by interaction between miR-137 and complementary sequences in the 3′ UTR of CSE1L. Immunohistochemistry revealed that CSE1L is upregulated in oligodendroglial tumors. Knockdown of CSE1L resulted in similar outcomes as overexpressing miR-137 in oligodendroglioma cells and glioblastoma cells. Overall, our data suggest that miR-137 regulates growth of glioma cells and targets CSE1L, providing further understanding in the tumorigenesis of gliomas.

INTRODUCTION

MicroRNAs (miRNAs) are a class of noncoding RNAs of 22–25 nucleotides in length that negatively regulate gene expression through complementary base pairing to their target messenger RNAs (5, 22). Recent studies have shown that dysregulation of miRNAs expression contributes to tumor development (9, 32). Several miRNAs have been reported to be aberrantly expressed in gliomas. For example, miR-21 is overexpressed in gliomas (13). Further studies demonstrated its involvement in cell motility, migration and apoptosis in gliomas and other cancers through negative regulation of PTEN, PDCD4, TIMP3 and TPM1 (14, 31, 45). Another miRNA, miR-7 is downregulated in gliomas (19, 37). Restoration of miR-7 leads to suppression of proliferation and invasion in glioblastoma (19). Similarly, miR-128 expression is reduced in gliomas. Ectopic miR-128 expression results in inhibition of glioma cell proliferation through targeting Bmi-1 and E2F3a (15, 44). These studies strongly suggest that miRNAs play a key role in the pathogenesis of gliomas.

MicroRNA-137 (miR-137) is a brain-enriched miRNA (23, 35, 38). Previously, two expression profiling studies demonstrated downregulation of miR-137 in high-grade astrocytic tumors (15, 36). However, functional characterization of miR-137 was not performed in these two studies, and the detailed roles of miR-137 in gliomagenesis remain to be elucidated. In this study, we demonstrate that miR-137 is downregulated in grades II and III oligodendroglial tumors and its expression is associated with tumor grade. Low miR-137 expression is also associated with shorter progressive-free survival and overall survival. We also show that miR-137 inhibits cell viability, anchorage-independent growth and invasion of glioma cells. Further investigation identifies that CSE1L is a target gene of miR-137, and suppression of CSE1L by siRNAs mimics the action of miR-137 in the inhibition of cell growth, anchorage-independent growth and invasion, indicating that the downregulation of miR-137 may be involved in gliomagenesis through potentiation of CSE1L expression.

MATERIALS AND METHODS

Tumor samples

A total of 35 oligodendroglial tumor samples, including 19 oligodendrogliomas (13 of grade II and six of grade III) and 16 oligoastrocytomas (13 of grade II and three of grade III), were studied. Histological classification was performed according to the current World Health Organization (WHO) criteria (29). Tissues

were collected from patients undergoing surgery for glioma. Tissues were stored in RNALater solution (Ambion, Austin, TX, USA) at –80°C until use. Histological review by pathologist confirmed all RNALater-preserved samples had tumor cell content greater than 80%. The mean age of patients was 41.9 years and the median was 41.0 years. The male/female ratio was 1.36:1. The clinical parameters of patients are summarized in Supporting Information Table S1.

Cell lines

Two human oligodendroglioma cell lines (HOG and TC620) and seven human glioblastoma multiforme (GBM) cell lines (A172, LNZ308, T98G, U118, U138, U373 and U87) were included in this study. HOG and TC620 cell lines were kind gifts from Dr. Glyn Dawson at University of Chicago, USA and Dr. Rainer Probstmeier at University of Bonn, Germany, respectively. A172, U118, U138, U373 and U87 cell lines were purchased from the American Type Culture Collection (ATCC, Rockville, MD, USA). All cell lines were cultured in recommended medium and housed in incubator at 37°C with 5% CO_2.

RNA extraction and quantitative reverse transcription polymerase chain reaction (RT-PCR)

Total RNA, including miRNA, was extracted from RNALater-stored tumor tissues and cell lines using TRIzol® reagent (Invitrogen, Carlsbad, CA, USA). Briefly, tissues were minced in TRIzol® and then subjected to homogenization. RNA isolation was continued according to manufacturer's instructions.

The stem-loop TaqMan miRNA assay (Applied Biosystems, Foster City, CA, USA) was employed to study miR-137 expression in tumor samples and normal brains. Briefly, a reverse transcriptase reaction mixture containing 20 ng total RNA samples, 1x miR-137-specific stem-loop RT primer, 1x RT buffer, 1 mM deoxyribonucleoside triphosphates (dNTPs), 50 U of MultiScribe™ reverse transcriptase and 3.8 U of RNase inhibitor was prepared. The reaction mixture was run for 30 min at 16°C, 30 min at 42°C and 5 min at 85°C. Quantitative PCR was conducted in a 10-μL volume contained 1/10 of the reversed transcribed product, 1 × TaqMan Universal PCR master mix, and 1 × TaqMan miRNA assay reagent. Amplification was performed at 95°C for 10 minutes, followed by 40 cycles of 95°C for 15 s, and 60°C for 1 minute on 7900HT Fast Real-Time PCR System (Applied Biosystems). Normalization was carried out using miR-16 which showed robust and consistent expression among normal brains and primary tumor samples. The expression of miR-137 level in tumor samples relative to controls was calculated using the comparative C_T ($2^{-\Delta\Delta CT}$) method. RNAs of five normal adult brain tissues served as control and they were obtained from BD Biosciences Clontech (Palo Alto, CA, USA), BioChain (Hayward, CA, USA) and Ambion (Austin, TX, USA). Three of the five normal RNA samples were obtained from whole brains and two of the normal RNA samples were obtained from frontal lobe of the brains as described by the manufacturers.

miR-137 transfection

The miRIDIAN hsa-miR-137 mimic (miR-137) and miRIDIAN miRNA mimic negative control (NC) were purchased from Dharmacon (Lafayette, CO, USA). Glioma cells ($7.5–10.0 \times 10^4$ cells) were plated sub-confluently on 6-well plate a day prior to transfection. Transfection was achieved using Lipofectamine™ 2000 (Invitrogen). A final concentration of 20 nM of miR-137 or NC was transfected into glioma cells. Transfection efficiency was monitored by siGLO Green transfection indicator (Dharmacon). Transfection conditions which resulted in >80% transfection efficiency was used in all experiments.

Cell viability count

Cell viability was determined by trypan blue exclusion assay. Glioma cells were subjected to miR-137, NC or mock (transfection reagent only) transfection. Cells were harvested by trypsinization, stained with 0.4% (w/v) trypan blue and counted with a hemocytometer. Assay was done in four consecutive days. The experiment was repeated three times independently. Each time, three measurements were taken for each sample.

5-Bromo-2′-deoxyuridine (BrdU) incorporation assay

BrdU incorporation was measured by Cell Proliferation ELISA BrdU kit (Roche Diagnostics GmbH, Mannheim, Germany) according to manufacturer's recommendation. At 72 h post-transfection, cells were labeled with BrdU for 45 minutes. Cells were then fixed with cold ethanol/HCl, stained with anti-BrdU antibody conjugated with peroxidase. Immune complexes were then detected by the subsequent substrate (tetramethylbenzidine) reaction, and were quantified by measuring the absorbance with spectrophotometer. The experiment was repeated three times independently. Three measurements of each sample were taken in each experiment.

Anchorage-independent growth assay

After transfection, cells were trypsinized, counted and suspended. A total of $2.0–4.0 \times 10^4$ cells in 0.3% agar were seeded on top of the 6-well plates. The bottom layers of plates were coated with 0.5% agar. Cells were incubated at 37°C for 3 weeks. Colonies were visualized by staining with crystal violet. Colonies were counted only when the diameter was greater than 1 mm. The experiment was repeated three times independently.

Matrigel invasion assay

Invasion assay was conducted with BD BioCoat™ Matrigel™ Invasion Chamber (BD Bioscience, Bedford, MA, USA) according to the manufacturer's protocol. Glioma cells were transfected with miR-137 or NC. At 48 h post-transfection, cells were trypsinized, counted and plated at a density of $1.0–2.0 \times 10^5$ cells per insert. After 16 h incubation, noninvading cells were removed. Invasive cells were fixed, stained with 1% toluidine blue (Sigma-Aldrich, St Louis, MO, USA) and counted. The experiment was repeated three times independently.

5-aza-2′-deoxycytidine (5-aza-dC) and Trichostatin A (TSA) treatment

5-aza-dC (Sigma-Aldrich) and TSA (Sigma-Aldrich) were dissolved in dimethyl sulfoxide (DMSO), and stored at –80°C until

used. For 5-aza-dC treatment, A172, TC620 and U373 cells were incubated at a concentration of 2, 5 or 10 μM for 96 h. The treatment with histone deacetylase inhibitor, TSA, was performed at 0.3 or 1 μM for 24 h. For combination study, 5-aza-dC was added for 96 h and TSA was then given for an additional of 24 h. Fresh media containing the drugs were changed every 24 h. Control cells were treated with 0.1% DMSO. Expression of miR-137 was measured by stem-loop-based RT-PCR as mentioned above. Three measurements were taken on each sample in every experiment. The experiment was repeated three times.

Luciferase vector construction

The 3′ UTR fragment of CSE1L was amplified using genomic DNA. The forward primer was 5′-AGAGTTACTAGTTAACCTGAACCTTGAGCAAA-3′, with dashed line representing nts 142–162 of 3'UTR of CSE1L. The reverse primer was 5′-AGAGTAAAGCTTAACCTGCCCTTAAGATGTTC-3′, with dashed line representing nts 512–522 of 3'UTR of CSE1L and double underline representing the genomic sequences followed the 3'UTR. Restriction sites SpeI and HindIII (underlined) were included for cloning purpose. Amplification product was first cloned into the pCR2.1-TOPO vector and then subcloned downstream of the firefly luciferase gene of pMIR-REPORTER luciferase vector (Ambion). The resultant plasmid was named pMIR-CSE1L WT. To generate a control vector, pMIR-CSE1L MUT, with 7-bp mutation at the putative binding site of miR-137, we utilized QuikChange Multi site-directed mutagenesis kit (Stratagene, La Jolla, CA, USA) according to the manufacturer's recommended protocol.

Dual luciferase assay

A day prior to transfection, $4.0–5.0 \times 10^4$ cells were seeded on a 24-well plate to achieve 90% confluence at transfection. On the day of transfection, a mixture containing 500 ng of pMIR-CSE1L WT or pMIR-CSE1L MUT plasmid, 100 ng of pRL-TK Renilla plasmid (Promega, Madison, WI, USA) and 10 pmol of miR-137 or NC were prepared and co-transfected into cells using 1 μL Lipofectamine 2000 (Invitrogen). Firefly and Renilla luciferase activities were measured at 48 h post-transfection using Dual-Glo® Luciferase Assay System (Promega) and a luminometer. The relative luciferase activity was calculated by the following steps. The Firefly luciferase activity was first normalized to the Renilla luciferase activity. The relative luciferase activity in negative control-transfected cells was set to 1, and the luciferase activity in miR-137 transfected cells was then calculated. Nontransfected cells were included for background subtraction. All experiments were conducted in triplicate and repeated three times.

Western blot analysis

Cells were collected, washed with ice-cold phosphate-buffered saline (PBS), lysed in RIPA buffer containing 50 mM Tris-HCI (pH 7.4), 150 mM NaCI, 1% NP-40, 0.1% sodium dodecyl sulfate (SDS) and 0.25% sodium deoxycholate, and 1X protease inhibitors. Protein lysates without debris were obtained by centrifugation and quantified by Protein Assay (Bio-Rad, Hercules, CA, USA). Soluble proteins were separated on SDS-polyacrylamide gel and transferred to Hybond-P polyvinylidene fluoride (PVDF) membrane (GE Healthcare, Buckinghamshire, UK). The blot was blocked with 5% nonfat milk, incubated with antihuman CSE1L monoclonal antibody 3D8 (Abnova, Jhongli City, Taoyuan County, Taiwan) at 5 μg/mL, or antihuman GAPDH monoclonal antibody (Abcam, Cambridge, UK) at 0.2 μg/mL, followed by horseradish peroxidase-conjugated sheep anti-mouse antibody. Proteins were then visualized by using SuperSignal West Pico Chemiluminescent Substrate (Thermo Scientific, Rockford, IL, USA). The experiment was repeated a minimum of three times.

Immunohistochemistry

Formalin-fixed and paraffin-embedded tissues were used, and 5-μm thick slide were deparaffinized in xylene, rehydrated in ethanol and antigens retrieved by microwave pretreatment in citrate buffer (10 mM citric acid, pH 6.0). Endogenous horseradish peroxidase (HRP) activity was inactivated with 3% hydrogen peroxide (H_2O_2) and the sections were then blocked with 2% normal swine serum. Then, primary CSE1L antibody 3D8 (Abnova) was applied at 1:50 dilution overnight at 4°C. The slides were then incubated with HRP labeled anti-mouse secondary antibody for 50 minutes. Immunoreactivity was visualized by diaminobenzidine (DAB) and counterstained with hematoxylin. PBS was used for rinsing between each step.

Histological expression of CSE1L was examined and graded by two investigators. Both cytoplasmic and nuclear staining was considered positive. The immunostaining result was then graded into three categories: weak (≤10% positive staining), moderate (10%–50% positive staining) and high (>50% positive staining).

Statistical analysis

Statistical analysis was conducted with the SPSS software version 16.0 (SPSS, Inc., Chicago, IL, USA). Kruskal–Wallis test was used to compare the relative miR-137 expression between normal brains, tumor samples and cell lines. Mann–Whitney *U*-test with Bonferroni correction was employed as *post hoc* analysis to compare the relative miR-137 expression between each two groups. Comparisons of cell number between different treatment groups were done by one-way analysis of variance (ANOVA) and *post hoc* analysis with Bonferroni correction. Student's *t*-test was used to compare results of continuous data between two groups. Association between categorical data was examined by Fisher's exact test. Kaplan–Meier survival analysis was used to examine overall survival (OS) and progression-free survival (PFS) and comparison was performed by log-rank test. Multivariate analysis was done by Cox-proportional hazards model. Results with *P*-value <0.05 were considered as statistically significant.

RESULTS

Reduced miR-137 expression in oligodendroglial tumors

To investigate miR-137 expression in gliomas, we applied stem-loop quantitative RT-PCR. In total, 35 tissue samples were studied, including 13 grade II oligodendrogliomas, 13 grade II oligoastrocytomas, six grade III anaplastic oligodendrogliomas and three grade III anaplastic oligoastrocytomas. We also included five

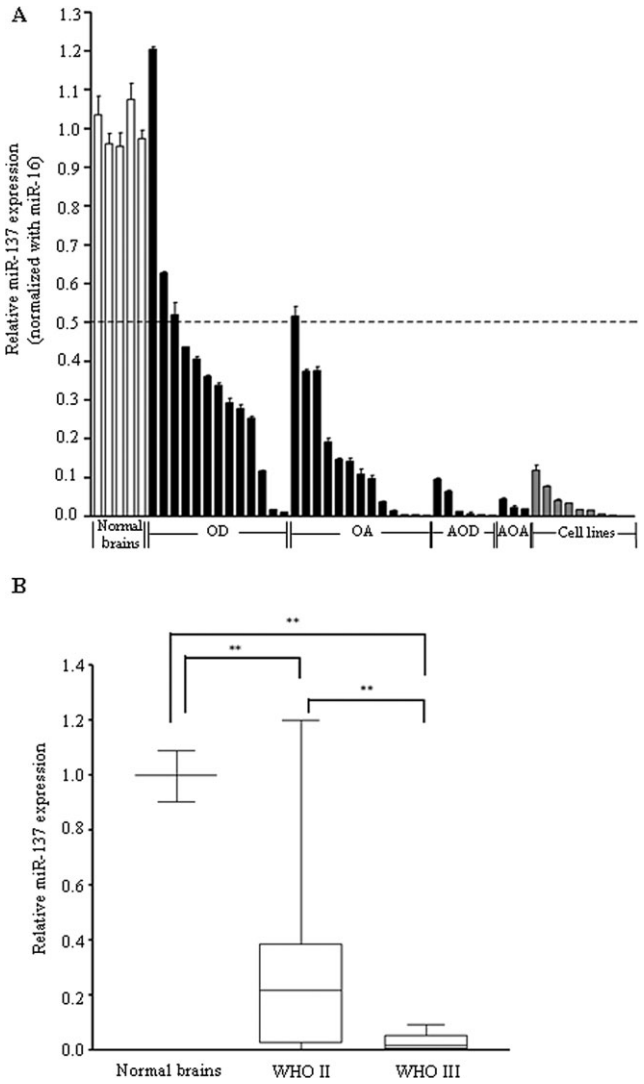

Figure 1. *Downregulation of miR-137 in oligodendroglial tumors.* **A.** Expression of miR-137 was evaluated by stem-loop qRT-PCR in 35 oligodendroglial tumors (black bar), nine glioma cell lines (gray bar) and five normal adult brains (white bar). Expression of miR-137 was normalized with miR-16 which showed a robust and consistent expression across samples. Dashed line represents twofold cutoff. **B.** Expression of miR-137 was significantly under-expressed in tumor samples compared with normal brains. When tumors were separated by grades, miR-137 expression was significantly reduced in grade III tumors compared with grade II tumors ($P < 0.01$).

normal brains as control. As shown in Figure 1A, 31/35 (88.6%) of tumor samples displayed a significant downregulation of miR-137 by at least twofold compared with the average of normal brains ($P < 0.001$, Mann–Whitney *U*-test). These included 22/26 (84.6%) grade II and 9/9 (100%) grade III tumors. Seventeen (48.6%) tumors exhibited a reduced miR-137 expression by >10-fold. There were three grade II oligodendrogliomas and one grade II oligoastrocytoma did not exhibit downregulation of miR-137 expression. When samples were separated according to their WHO grades, grade II tumors ($P < 0.001$, Mann–Whitney *U*-test) and grade III tumors ($P < 0.001$, Mann–Whitney *U*-test) showed significantly reduced miR-137 expression compared with that of normal brains. The expression level of miR-137 was significantly lower in grade III tumors compared with grade II tumors (Figure 1B; $P = 0.005$, Mann–Whitney *U*-test). We also determined miR-137 expression in a panel of human oligodendroglioma and also glioblastoma cell lines as few oligodendroglioma cell lines are available. All nine of

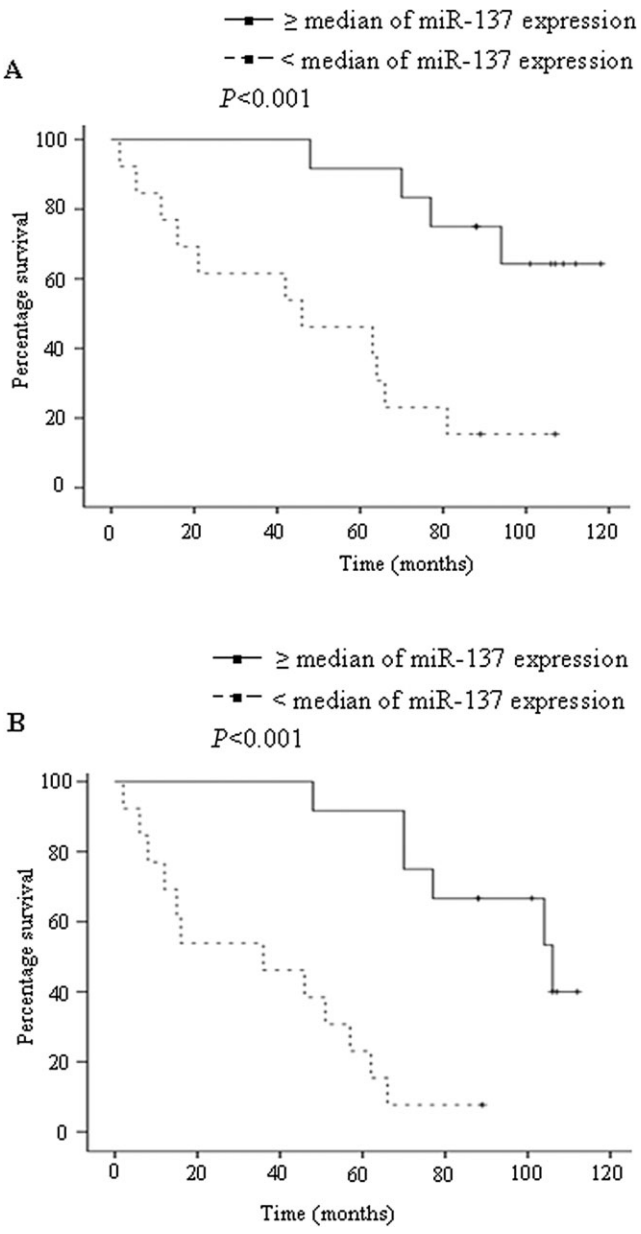

Figure 2. *Kaplan–Meier analysis for overall survival and progression-free survival in 25 glioma patients.* **A.** Tumors with <median of miR-137 expression were associated with shorter overall survival and **B.** progression-free survival. The median value of miR-137 level was chosen as cutoff to separate miR-137 low-expression tumors ($n = 13$) from miR-137 high-expression tumor ($n = 12$). *P*-value was obtained with the use of log-rank test.

them displayed significant downregulation of miR-137 expression compared with normal brains (Figure 1A).

Next, we evaluated the prognostic significances of miR-137 expression and various clinical parameters. Survival data was available in 25 cases. Kaplan–Meier survival analysis revealed age above 50 years old ($P = 0.005$) and WHO grade III tumors ($P < 0.001$) were associated with shorter OS (Supporting Information Figure S1A and B). Oligoastrocytic phenotype showed a trend toward shorter OS ($P = 0.05$; Supporting Information Figure S1C). Age above 50 years old ($P = 0.031$) and grade III tumors ($P < 0.001$) but not oligoastrocytic phenotype were associated with shorter PFS (Supporting Information Figure S1D–F). To investigate the prognostic value of miR-137 expression, patients were separated into two groups: tumors with <median of miR-137 expression and tumors with ≥ median of miR-137 expression. As shown in Figure 2A and B, patients with < median of miR-137 expression had shorter OS ($P < 0.001$, median OS = 46 months vs. not reached) and PFS ($P < 0.001$, median PFS = 36 months vs. 106 months). Out of 13 tumors displayed < median of miR-137 expression, six of them were grade II tumors and seven of them were grade III tumors. Yet, none of the grade III tumors had ≥ median of miR-137 expression ($P = 0.005$, Fisher's exact test). To avoid the confounding effect of WHO grading, we re-examined survival data to include 18 grade II patients with survival data available. Kaplan–Meier survival analysis demonstrated that patients with < median of miR-137 expression had shorter PFS than those with ≥ median

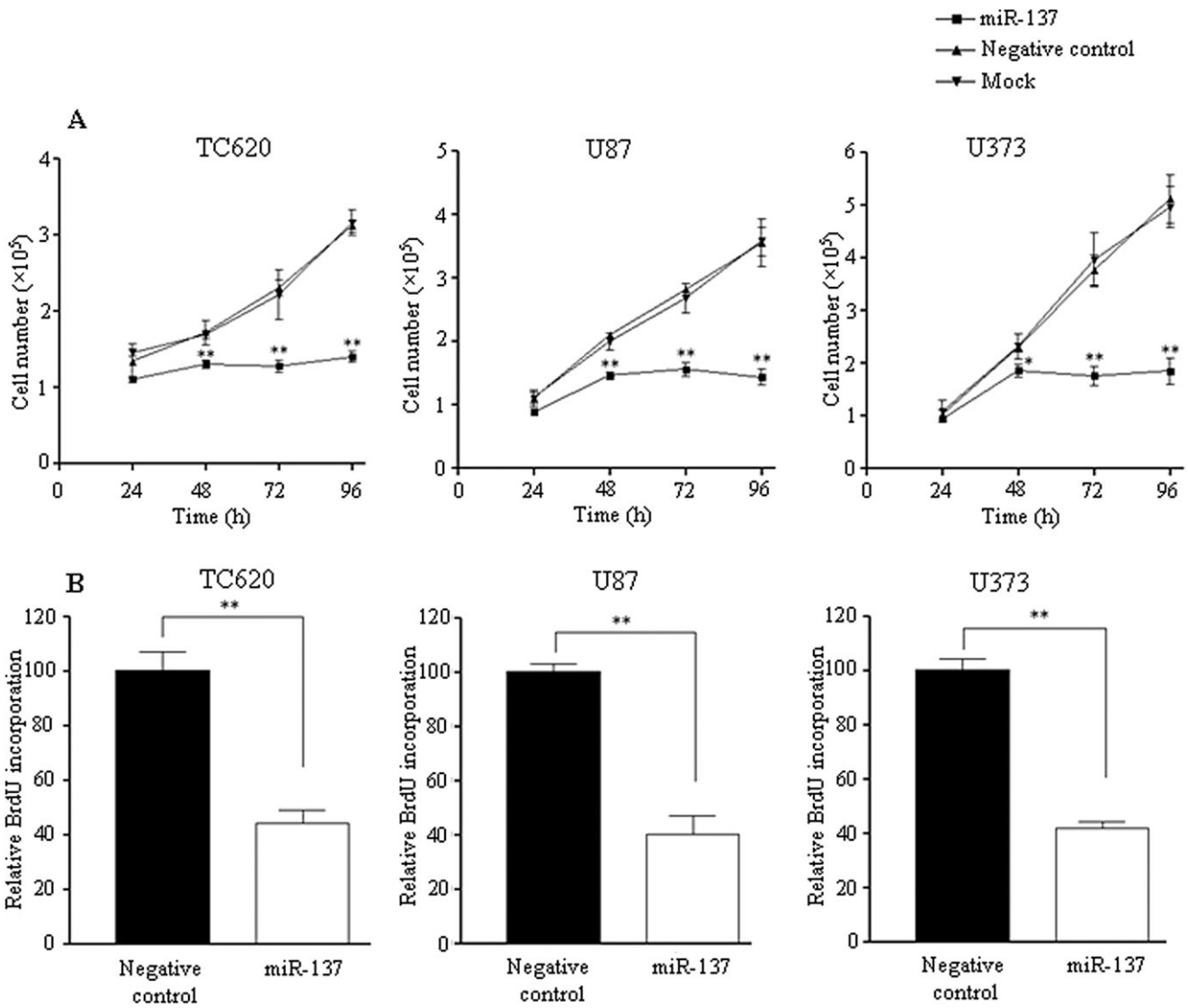

Figure 3. *Ectopic miR-137 expression reduced cell growth and proliferation.* **A.** TC620 (left), U87 (middle) and U373 (right) cells were transfected with miR-137, negative control or mock. Cell viability was determined by trypan blue cell counting. Significant growth inhibition of growth was observed at 48, 72 and 96 h post-transfection as analyzed by one-way ANOVA. **B.** Proliferation was measured by incorporation of the thymidine analog BrdU. Compared with the negative control-transfected cells, miR-137-transfected glioma cells displayed marked attenuation in BrdU incorporation. $*P < 0.05$; $**P < 0.01$.

of miR-137 expression (Supporting Information Figure S2B, $P = 0.007$, median PFS = 57 months vs. 106 months). No significant association between OS of grade II tumor and miR-137 expression was achieved (Supporting Information Figure S2A). We did not observe a correlation between miR-137 expression and other clinical parameters including sex and chromosome 1p/19q status; the latter was routinely examined by fluorescence *in situ* hybridization (FISH) in our laboratory.

Taken together, miR-137 downregulation is a frequent event in oligodendroglial tumors and glioma cell lines. In our cohort of samples, grade III tumors showed further reduced miR-137 expression compared with grade II tumors. MiR-137 downregulation was also associated with shorter OS and PFS, suggesting it is a potential prognostic marker in oligodendroglial tumors.

miR-137 suppress cell viability and proliferation

Again, because of a paucity of studies on oligodendroglioma cell lines, we transiently transfected miR-137 mimic in an oligodendroglioma cell line, TC620, as well as two GBM cell lines, U87 and U373. All of them expressed minimal level of miR-137. Cell viability was examined by trypan blue exclusion test for four consecutive days. Ectopic miR-137 expression led to a significant suppression in the cell number of glioma cells (Figure 3A). Compared with negative control-transfected cells, cell viability in miR-137-transfected TC620 cells was decreased by 24.2% at 48 h, and further decreased by 44.8% and 55.0% at 72 h and 96 h, respectively. Restoration of miR-137 in U87 cells reduced cell viability by 30.5% at 48 h, 44.8% at 72 h and 59.7% at 96 h. Cell viability in miR-137-expressed U373 cells was suppressed by 19.0% at 48 h, 53.4 % at 72 h and 64.0% at 96 h. There was no significant difference in cell viability between negative control and mock-transfected cells. By BrdU incorporation assay, we also confirmed that cell growth suppression was likely a result of a decrease in cell proliferation. Figure 3B illustrated that BrdU incorporation in miR-137-transfected TC620 cells was markedly reduced compared with negative controls at 48 h post-transfection ($P < 0.01$, Student's *t*-test). Consistent findings were observed in the two other gliomas cells.

miR-137 impaired anchorage-independent growth

We then investigated the effect of miR-137 on anchorage-independent growth of glioma cells. As illustrated in Figure 4A

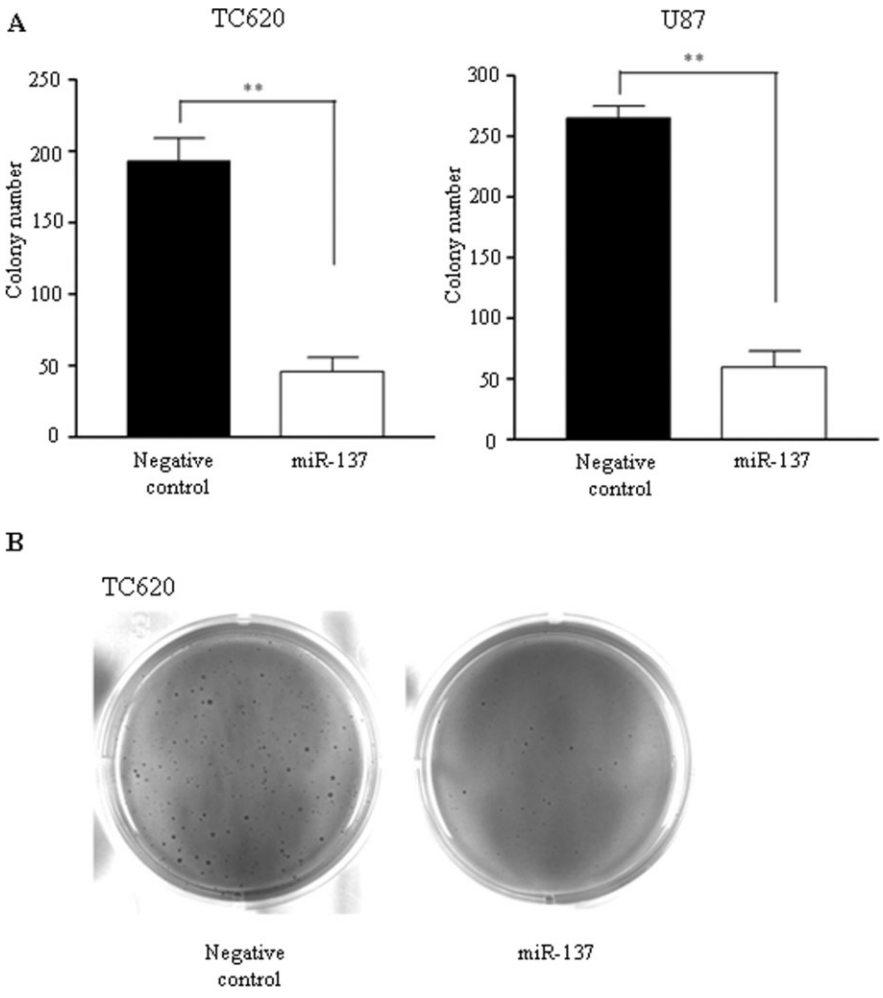

Figure 4. *Suppression of colony formation efficiency in glioma cells by miR-137.*
A. TC620 and U87 cells were transfected with miR-137 or negative control and grown in soft agar for 21 days. The bars represent the average of number of colonies formed in three independent experiments.
B. Photographs of stained soft agar plates of TC620 cells.

and B, miR-137 restoration in TC620 and U87 cells resulted in a pronounced reduction of colony forming ability ($P < 0.01$). At 21 days after incubation, the number of colonies formed by TC620 cells was decreased from 193 ± 16 to 46 ± 10 and the number of colonies formed by U87 cells was decreased from 265 ± 10 to 59 ± 14. These results further suggested that miR-137 might be an important regulator of glioma cell growth. U373 cells were not included in colony formation assay because of its inability to form colony.

miR-137 inhibited cell invasion

To explore if miR-137 would have an effect on tumor invasion, we conducted *in vitro* Matrigel invasion assay. The result revealed that invasion through extracellular matrix was remarkably decreased in miR-137-transfected glioma cells as compared with negative controls (Figure 5, $P < 0.05$). Compared with negative controls, at 48 h after miR-137 transfection, the number of cells passing through the matrix was attenuated by 38.9% in TC620, 47.9% in U87 and 54.8% in U373 cells. These results suggest that miR-137 plays an important role in the suppression of invasion of glioma cells.

Demethylation and deacetylation treatments in glioma cells

Previous studies have indicated that the importance of miR-137 promoter hypermethylation in oral squamous cell carcinoma, gastric cancer and colorectal cancer, and demethylation treatment would restore miR-137 expression (4, 11, 20, 24). To examine the potential role of epigenetic regulation of miR-137 expression in glioma, three cell lines were treated with DNA methyltransferase inhibitor, 5-aza-dC, histone deacetylase inhibitor, TSA, or in combination. Expression of miR-137 was then examined by stem-loop-based RT-PCR. As shown in Figure 6A, miR-137 expression in TC620 cells was prominently elevated upon treatment with 5-aza-dC, or a combination of 5-aza-dC and TSA ($P < 0.01$; one-way ANOVA). Treatment with 10 μM 5-aza-dC in TC620 cells resulted in an upregulation of miR-137 expression by 9.6-fold compared with control cells. Both 5-aza-dC and TSA treatment in TC620 cells significantly increased miR-137 expression by 11.2- to 17.4-fold compared with control cells. However, induction of miR-137 expression was not detected in A172 and U373 cells upon demethylation and/or deacetylation treatment (Figure 6B and C). Taken together, epigenetic regulation might involve in controlling miR-137 expression in a small subset of glioma cells.

Identification of miR-137 targets

To identify potential miR-137 targets that may be implicated in gliomagenesis, we retrieved databases from three *in silico* microRNA target prediction algorithms, namely miRanda, PicTar and TargetScan. We then searched for potential miR-137 target genes that fell into the following criteria. First, the putative target genes had to be predicted by at least two computational algorithms. Second, the complementary base pairings at the seed region between miR-137 and target genes had to be well conserved across species. Third, the putative target genes had to be implicated in gliomagenesis, and they had to be shown to play a role in proliferation, apoptosis or invasion. By these criteria, we narrowed down to four genes, namely, CSE1 chromosome segregation 1-like (CSE1L), cell division cycle 42 (CDC42), neuropilin 1 (NRP1) and v-akt murine thymoma viral oncogene homolog 2 (AKT2). Bioinformatic tools identified one potential binding site of miR-137 on 3'UTRs of CSE1L, CDC42 and NRP1. Furthermore, two complimentary binding sites of miR-137 were found

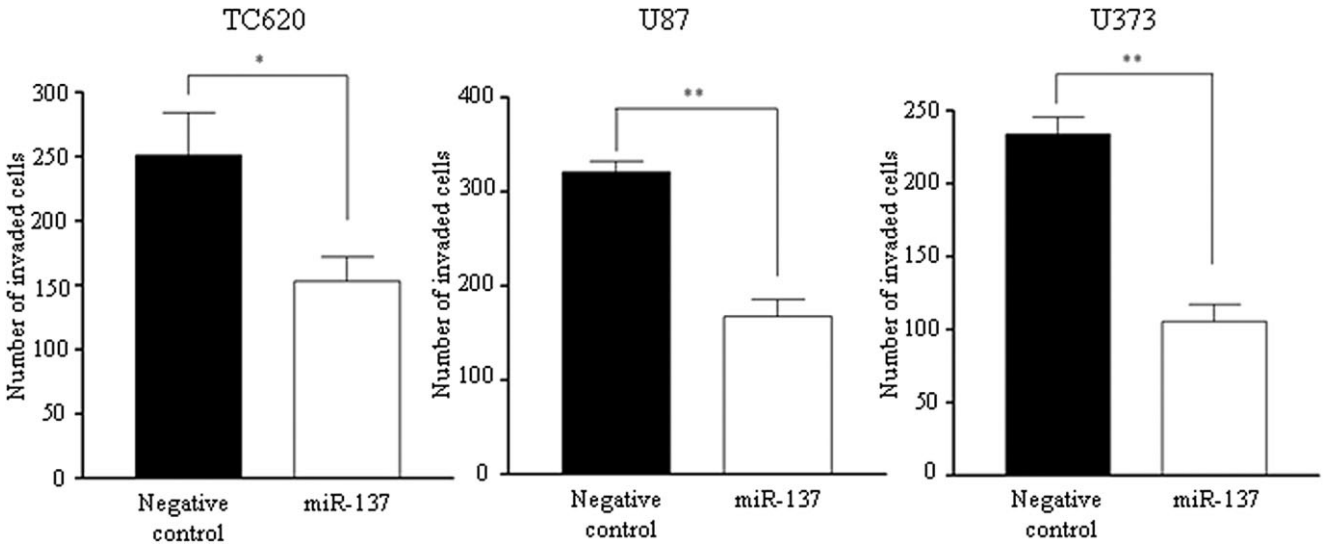

Figure 5. *Ectopic miR-137 expression decreased cell invasion.* Three glioma cells were transfected with miR-137 or negative control. The effect of miR-137 on cell invasion was assessed by matrigel invasion assay. The bars represent the average number of cells passing through the inserts in three separate experiments.

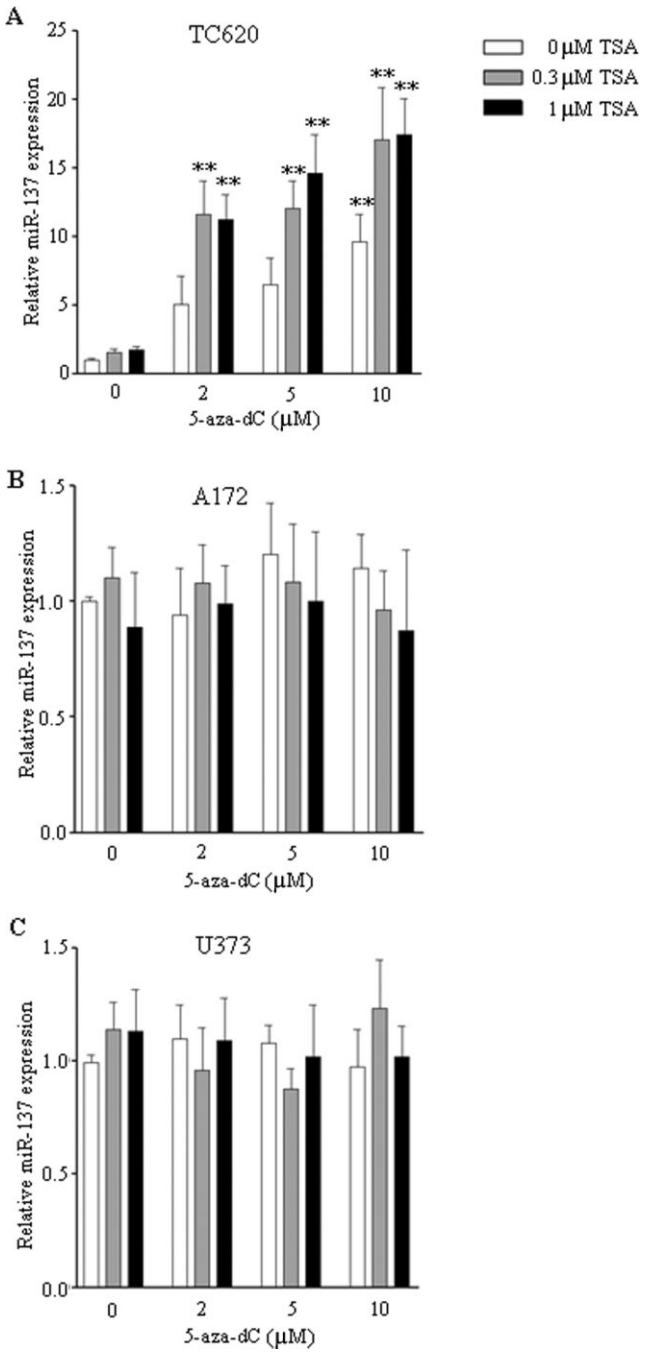

Figure 6. *Expression of miR-137 in glioma cells upon demethylation and/or deacetylation treatment.* Glioma cells were treated with 5-aza-dC, TSA or combination as described in Materials and Methods. Expression of miR-137 was assessed by quantitative RT-PCR. **A.** Expression of miR-137 was upregulated in TC620 cells upon 5-aza-dC or combination of 5-aza-dC and TSA. **B, C.** An increase of miR-137 expression was not detected in A172 (**B**) and U373 (**C**) cells upon treatment. The bars represent the average of relative miR-137 expression derived from three separate experiments. $^{**}P < 0.01$.

within 3'UTR of AKT2, and they were separated by approximately 1000 bps.

CSE1L is the target gene of miR-137

To test the direct interaction of these putative target genes and miR-137, we amplified 3'UTR sequences of CSE1L, CDC42 and NRP1 and inserted them downstream of the firefly luciferase coding region of pMIR-REPORT vectors. Furthermore, the 3'UTR of AKT2 was amplified into two fragments with each of them containing one potential binding site of miR-137. They were then cloned into pMIR-REPORT vectors. The dual luciferase assay revealed that the relative luciferase activity was remarkably repressed by 44.0% when LNZ308 cells were co-transfected with miR-137 and a luciferase plasmid bearing 3'UTR of CSE1L (pMIR-CSElL WT, Figure 7A). We then prepared a mutant construct in which the 7-bp putative binding site at the 3′ UTR of CSE1L was changed (pMIR-CSE1L MUT). Transient co-transfection of LNZ308 cells with this mutant plasmid and miR-137 did not result in a significant alteration in relative luciferase activity (Figure 7A). These results suggested a direct interaction between miR-137 and putative binding site on CSE1L. Sequence analysis indicated that miR-137 formed complementary base pairing at nucleotides 482–488 of CSE1L 3'UTR, and miR-137 binding site on 3'UTR of CSE1L was conserved across eight species (Figure 7B). Furthermore, a significant change in luciferase activity was not observed when LNZ308 cells were co-transfected with miR-137 and reporter constructs containing 3'UTRs of CDC42, NRP1 or AKT2, suggesting these genes were unlikely the direct targets of miR-137 (Supporting Information Figure S3).

miR-137 downregulated CSE1L

We then applied Western blot analysis to provide further evidence for CSE1L as a target gene of miR-137. Seven gliomas cell lines were transfected with either miR-137 or negative control and cell lysates were collected at 48 h post-transfection. As illustrated in Figure 7C, CSE1L protein expression was substantially diminished upon miR-137 expression. We also quantified CSE1L transcript level by quantitative RT-PCR. Expression of CSE1L was not significantly changed in miR-137-transfected cells as compared with negative control cells (data not shown). The results suggested that miR-137 targeted CSE1L and regulated its expression at translation level.

CSE1L is upregulated in oligodendroglial tumors

We then studied expression of CSE1L by immunohistochemistry in our cohort of oligodendroglial tumors. With the exception of one oligoastrocytoma, all tumor samples had paraffin-embedded slide available. We also included 13 nontumor brain tissue samples. CSE1L scoring was graded into weak, moderate and strong according to the percentage of cells with positive staining. In nontumor brain tissue samples, weak CSE1L staining was observed in 11/13 (84.6%) samples (Figure 8A and E). Moderate staining was displayed in 2/13 (15.4%) and none of the cases had strong staining. Both glial and neuronal cells of nontumor brain

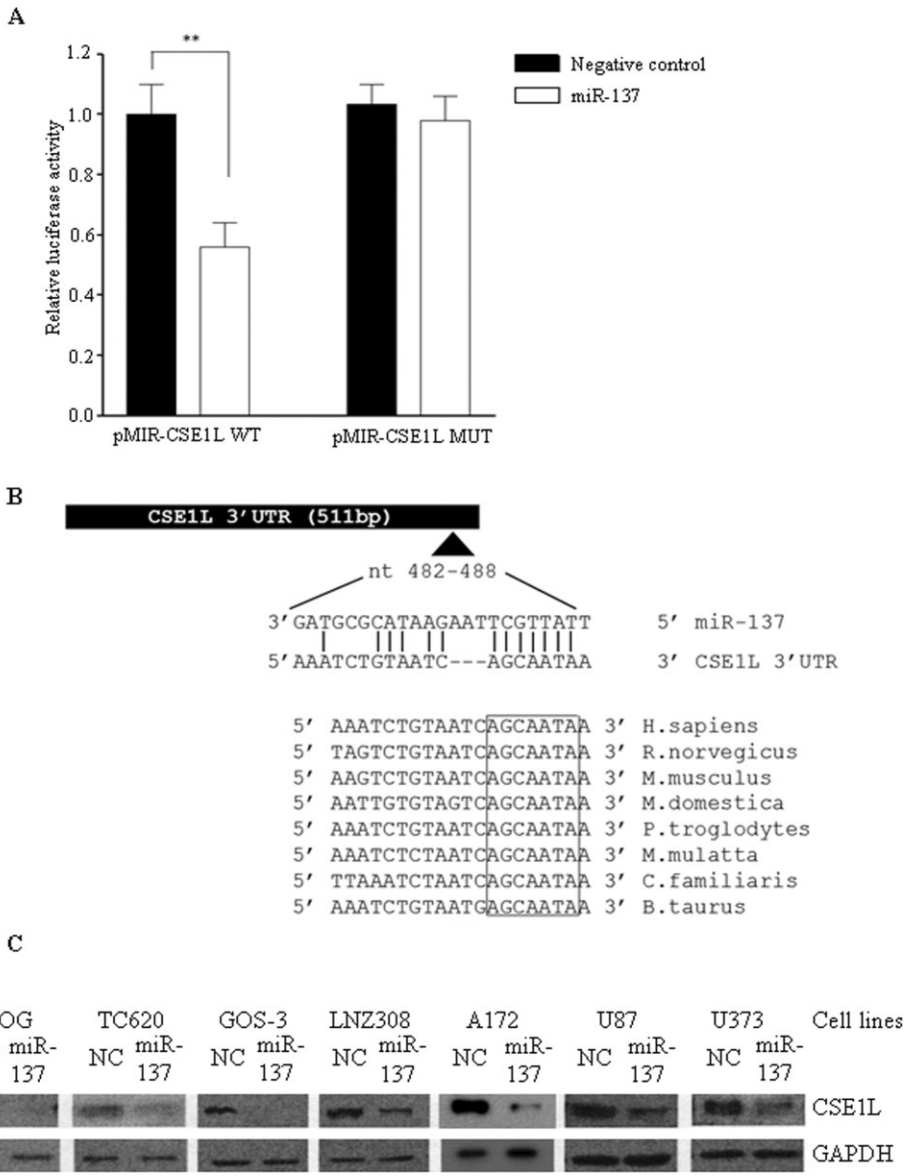

Figure 7. *CSE1L is a direct target of miR-137.* **A.** Luciferase reporter assay illustrated that miR-137 directly interacted with 3′UTR of CSE1L. LNZ308 cells were co-transfected with luciferase reporter constructs bearing 3′UTR of CSE1L (pMIR-CSE1L WT), miR-137 or negative control. In parallel, a mutant luciferase reporter plasmid with 7-bp change at the seed region (pMIR-CSEIL MUT) was prepared. **B.** A schematic diagram showing the potential miR-137 binding site on 3′UTR of human CSE1L. The binding site of miR-137 is conserved across eight species. **C.** CSE1L expression was markedly downregulated in miR-137 overexpressed cells as shown by Western blot analysis. A total of seven glioma cell lines were examined.

tissues showed positive staining of CSE1L. In contrast, increased CSE1L expression was observed in gliomas. Immunohistochemistry revealed that 6/34 (17.6%) tumor samples exhibited weak CSE1L staining (Figure 8B). Moderate and strong CSE1L staining was found in 12/34 (35.3%) and 16/34 (47.1%) cases, respectively (Figure 8C and D). Statistical analysis revealed that CSE1L expression was differentially expressed in oligodendroglial tumors compared with nontumor brains (Figure 8E, $P < 0.01$). However, we did not observe a correlation between CSE1L and miR-137 expression. Also, CSE1L immunostaining was not associated with clinical parameters and outcomes.

Depletion of CSE1L resulted in phenomena similar to that of miR-137 restoration

To carry out functional characterization of CSE1L in gliomas, we delivered two CSE1L specific siRNAs in TC620, U87 and U373 cells. In the initial study, we included mock and negative control for siRNA, and we did not observe a difference. Subsequent experiments were carried out with negative control. The efficacy of two siRNAs against CSE1L was confirmed by Western blot analysis (Supporting Information Figure S4). The effect of silencing CSE1L on cell viability was measured by trypan blue assay for

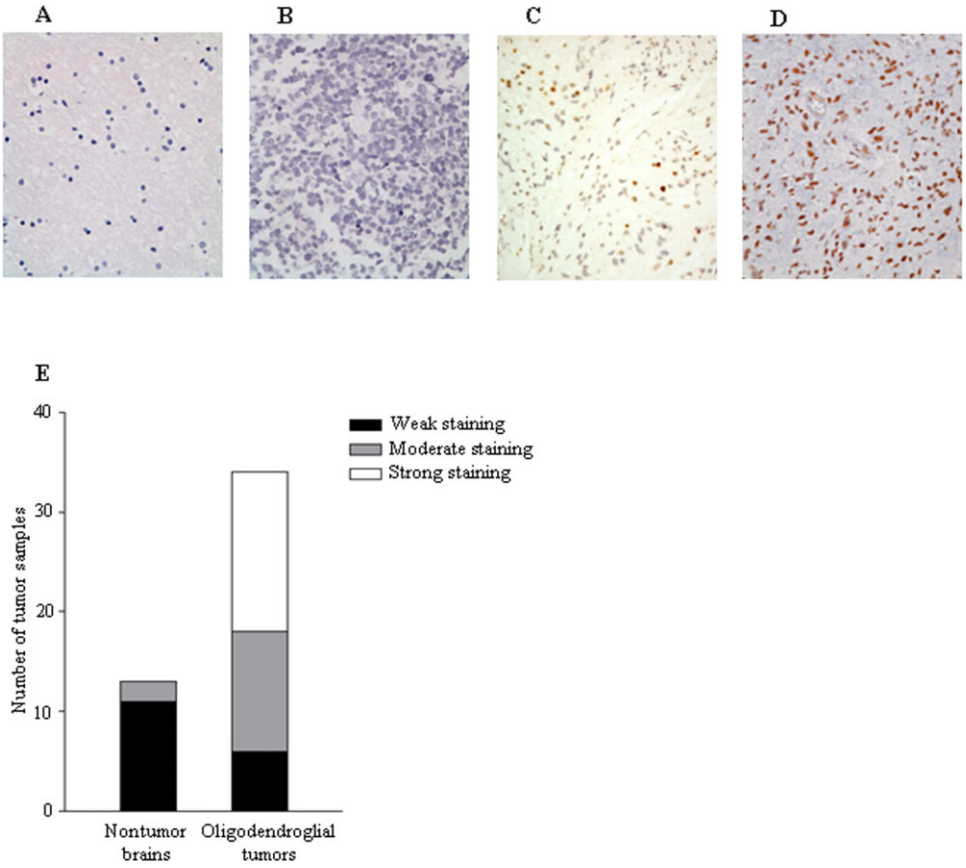

Figure 8. *Upregulation of CSE1L in oligodendroglial tumors.* Examples of (**A**) weak staining on a nontumor brain tissue, (**B**) weak staining, (**C**) moderate staining and (**D**) strong staining on oligodendroglial tumors. (**E**) Increased CSE1L expression was detected in oligodendroglial tumors compared with nontumor brain tissues.

four consecutive days. CSE1L depletion led to a significant suppression in cell viability (Figure 9A). Further analysis of DNA synthesis by BrdU incorporation assay suggested that knockdown of CSE1L led to reduction in cell proliferation (data not shown). Colony formation assay revealed that depletion of CSE1L impaired the ability of TC620 and U87 cells to grow in semisolid media (Figure 9B). In addition, transwell assay with Matrigel showed that invasive capacities were dramatically suppressed in miR-137-transfected cells compared with negative control-transfected cells (Figure 9C). These results were similar to that of overexpression of miR-137, suggesting that miR-137 inhibits growth of glioma cells by negatively regulating CSE1L expression.

DISCUSSION

MiRNAs are an emerging class of small noncoding RNAs, which post-transcriptionally regulate a large number of genes (8, 30). Aberrant miRNA expression has been identified in various cancers including brain, breast, gastric and prostate cancers (17, 25, 27, 39, 43). We hypothesized that dysregulation of miRNAs would be important for gliomagenesis. Previous studies have demonstrated that miRNAs are expressed in a tissue or cell type specific manner (23, 26). MiR-137 is a brain-enriched miRNA (23, 35, 38). It has been shown to be downregulated in high-grade astrocytic tumors in two expression profiling studies but there is little information available concerning its functional role or its significance, especially in oligodendroglial tumors (14, 36). In the present study, we delineated the expression pattern, clinical significance and biological functions of miR-137 in oligodendrogliomas and glioma cells. The key finding in this study is that downregulation of miR-137 is a frequent event in oligodendroglial tumors. In our cohort of grade II and grade III oligodendroglial tumors, 31/35 (88.6%) showed reduction in miR-137 expression more than twofolds compared with normal adult brains. Statistical analysis showed that aberrant miR-137 expression was significantly correlated with advanced tumor grade. Our results are consistent with previous studies showing downregulation of miR-137 in glioma (10, 15, 36). Furthermore, in our cohort of patients, patients with < median of miR-137 expression had a significantly shorter OS and PFS than those with ≥ median of miR-137 expression. The facts that < median of miR-137 expression was more frequently observed in high tumor grade and our sample size was small, the prognostic value of miR-137 expression in oligodendroglial tumors remains to be elucidated. Further investigation with large sample sizes is needed.

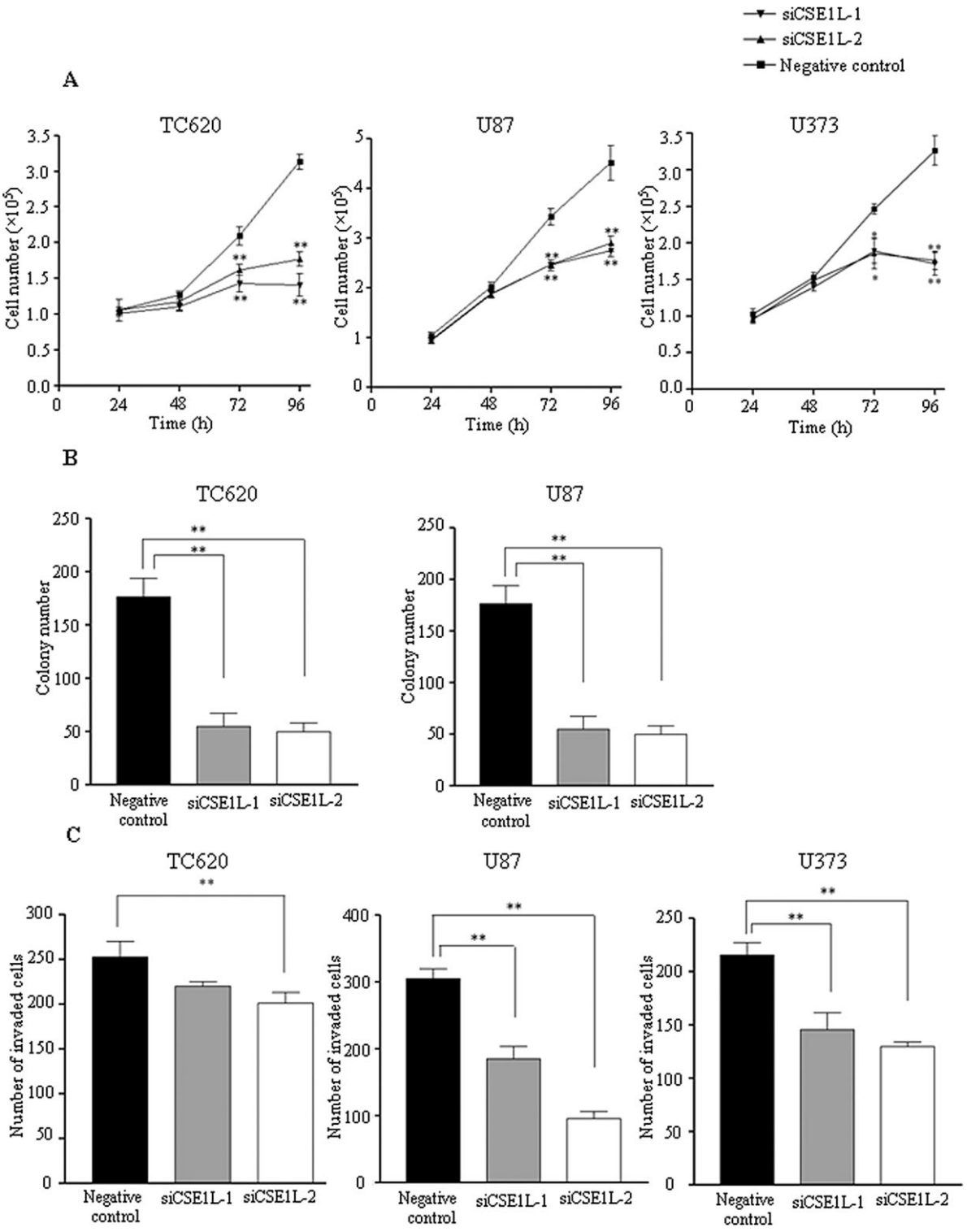

Figure 9. *Effects of CSE1L depletion on cell viability, colony formation and invasion of glioma cell lines.* **A.** Knockdown CSE1L significant suppressed cell growth of glioma cells. **B.** The number of colony formation in soft agar was markedly suppressed in CSE1L-knockdown TC620 and U87 cells compared with negative control-transfected cells. **C.** The number of cells passing through the inserts was significantly decreased in CSE1L depleted glioma cells. The experiment was repeated three times. $*P < 0.05$; $**P < 0.01$.

There have been two studies on the roles of miR-137 in gliomas. One was conducted by Chen *et al* showing the effects of miR-137 on the growth and invasion of GBM cells (10). The other one was carried out by Silber *et al* showing the inhibitory effect of miR-137 on cell proliferation of GBM cells (36). Our data showing the suppressive effects of miR-137 on cell growth, DNA synthesis and invasion ability of glioma cells extended the findings of these studies. More importantly, ours is the first to report on the functional roles of miR-137 in oligodendroglial tumors. In addition, we demonstrated that miR-137 would attenuate colony formation ability of both oligodendroglioma and glioma cells. Our data on the effects of miR-137 on cell viability, anchorage-independent growth and invasion ability strongly support that miR-137 exhibits a growth suppressive function in gliomas.

Prediction of miRNA target is a challenging task because of the imperfect duplexes formed between a given miRNA and its targets and the fact that gene expression is tissue specific and/or time specific (5). In the current study, we identified CSE1L as a direct target of miR-137. Luciferase reporter assay and mutational studies verified that miR-137 targeted the seed matching region at the 3'UTR of CSE1L. Ectopic expression of miR-137 in glioma cells resulted in marked reduction of CSE1L expression without affecting the mRNA level, suggesting that miR-137 regulates CSE1L post-transcriptionally. CSE1L expression was also upregulated in our cohort of oligodendroglial tumors. We showed that miR-137 downregulation is a new mechanism responsible for CSE1L activation. We did not, however, observe a strict inverse correlation between miR-137 expression and CSE1L expression in individual tumor samples. A plausible explanation is that CSE1L is potentially regulated by multiple miRNAs. This is supported by computational prediction analysis showing that binding sites for miR-23a, -23b, -31, -128, -182, -335 and -377 are found at 3'UTR of CSE1L. A second possible explanation is chromosomal aberration of 20q13, where CSE1L is located. Chromosomal gain of 20q13 is common in various tumors (1, 33). We have also previously reported on the high frequency of CSE1L amplification in gliomas (16). Another postulated explanation is that CSE1L expression was also subjected to hepatocyte growth factor (HGF)/Met signaling activation and interferon-gamma treatment (18, 34).

CSE1L is the human homolog of the yeast chromosome segregation gene, CSE1 (7). It encodes a 971-amino acid protein with a protein size of approximately 100 kDa. The protein is located in both cytoplasm and nuclei of cells (7). CSE1L is known to play roles in multiple biological functions. For instance, CSE1L is critical in mitotic spindle checkpoint and in maintenance of genomic stability (6). It is also involved in nuclear-cytolasmic reshuffling of importin-α, fluid secretion, migration and regulation of p53 target genes (2, 21, 40, 41). Earlier studies have reported that cell viability was decreased in colon and ovarian cancer cells upon CSE1L depletion (1, 28). In line with these results, we have showed in this study that depletion of CSE1L led to growth suppression of glioma cells. In addition, we are the first to report that anchorage-independent cell growth and cell invasiveness are retarded in CSE1L-depleted glioma cells. More importantly, we have shown that CSE1L knockdown would recapitulate the biological effects of miR-137 overexpression in glioma cells, suggesting that the growth suppressive function of miR-137 may be subjected to regulation by CSE1L.

Epigenetic silencing of miR-137 expression had been identified in multiple tumors, including colorectal, gastric and oral squamous cell carcinoma (3, 4, 11, 42). Demethylation and deacetylation treatment of uveal melanoma cell line resulted in an increase in miR-137 expression (12). These results prompted us to investigate the epigenetic regulation of miR-137 in gliomas. We have found that upregulation of miR-137 expression by 5-aza-dC and TSA treatment was only observed in TC620 oligodendroglioma cells while two GBM cell lines did not respond. Although the current results suggest that DNA methylation may not be a major mechanism for dysregulation of miR-137 in gliomas, they merit further investigations to delineate the epigenetic control in regulating miR-137 expression of gliomas.

In conclusion, we have demonstrated that dysregulation of miR-137 is a common feature in oligodendroglial tumors. We have showed that expression of miR-137 is associated with OS and PFS in our cohort of samples, suggesting a potential prognostic value of miR-137 in oligodendroglial tumors. Our data has also established a growth suppressive role of miR-137 in gliomas. Expression of miR-137 inhibits cell survival, proliferation, colony formation and invasive potential. Taken together, our data help to enhance the understanding tumorigenesis of oligodendroglial tumors.

FUNDING

This study is partially supported by a grant from the Natural Science Foundation, China.

CONFLICT OF INTEREST

The authors declare that they have no conflict of interest.

REFERENCES

1. Alnabulsi A, Agouni A, Mitra S, Garcia-Murillas I, Carpenter B, Bird S, Murray GI (2012) Cellular apoptosis susceptibility (chromosome segregation 1-like, CSE1L) gene is a key regulator of apoptosis, migration and invasion in colorectal cancer. *J Pathol* **228**:471–481. doi:10.1002/path.4031.
2. Bagnat M, Navis A, Herbstreith S, Brand-Arzamendi K, Curado S, Gabriel S *et al* (2010) Cse1l is a negative regulator of CFTR-dependent fluid secretion. *Curr Biol* **20**:1840–1845.
3. Balaguer F, Link A, Lozano JJ, Cuatrecasas M, Nagasaka T, Boland CR, Goel A (2010) Epigenetic silencing of miR-137 is an early event in colorectal carcinogenesis. *Cancer Res* **70**: 6609–6618.
4. Bandres E, Agirre X, Bitarte N, Ramirez N, Zarate R, Roman-Gomez J *et al* (2009) Epigenetic regulation of microRNA expression in colorectal cancer. *Int J Cancer* **125**:2737–2743.
5. Bartel DP (2004) MicroRNAs: genomics, biogenesis, mechanism, and function. *Cell* **116**:281–297.
6. Brinkmann U (1998) CAS, the human homologue of the yeast chromosome-segregation gene CSE1, in proliferation, apoptosis, and cancer. *Am J Hum Genet* **62**:509–513.
7. Brinkmann U, Brinkmann E, Gallo M, Pastan I (1995) Cloning and characterization of a cellular apoptosis susceptibility gene, the human homologue to the yeast chromosome segregation gene CSE1. *Proc Natl Acad Sci U S A* **92**:10427–10431.
8. Calin GA, Croce CM (2006) MicroRNA signatures in human cancers. *Nat Rev Cancer* **6**:857–866.

9. Calin GA, Liu CG, Sevignani C, Ferracin M, Felli N, Dumitru CD *et al* (2004) MicroRNA profiling reveals distinct signatures in B cell chronic lymphocytic leukemias. *Proc Natl Acad Sci U S A* **101**:11755–11760.
10. Chen L, Wang X, Wang H, Li Y, Yan W, Han L *et al* (2012) miR-137 is frequently down-regulated in glioblastoma and is a negative regulator of Cox-2. *Eur J Cancer* **48**:3104–3111. doi:10.1016/j.ejca.2012.02.007.
11. Chen Q, Chen X, Zhang M, Fan Q, Luo S, Cao X (2011a) miR-137 is frequently down-regulated in gastric cancer and is a negative regulator of Cdc42. *Dig Dis Sci* **56**:2009–2016.
12. Chen X, Wang J, Shen H, Lu J, Li C, Hu DN *et al* (2011b) Epigenetics, microRNAs, and carcinogenesis: functional role of microRNA-137 in uveal melanoma. *Invest Ophthalmol Vis Sci* **52**:1193–1199.
13. Conti A, Aguennouz M, La Torre D, Tomasello C, Cardali S, Angileri FF *et al* (2009) miR-21 and 221 upregulation and miR-181b downregulation in human grade II-IV astrocytic tumors. *J Neurooncol* **93**:325–332.
14. Gabriely G, Wurdinger T, Kesari S, Esau CC, Burchard J, Linsley PS, Krichevsky AM (2008) MicroRNA 21 promotes glioma invasion by targeting matrix metalloproteinase regulators. *Mol Cell Biol* **28**:5369–5380.
15. Godlewski J, Nowicki MO, Bronisz A, Williams S, Otsuki A, Nuovo G *et al* (2008) Targeting of the Bmi-1 oncogene/stem cell renewal factor by microRNA-128 inhibits glioma proliferation and self-renewal. *Cancer Res* **68**:9125–9130.
16. Hui AB, Lo KW, Yin XL, Poon WS, Ng HK (2001) Detection of multiple gene amplifications in glioblastoma multiforme using array-based comparative genomic hybridization. *Lab Invest* **81**:717–723.
17. Iorio MV, Ferracin M, Liu CG, Veronese A, Spizzo R, Sabbioni S *et al* (2005) MicroRNA gene expression deregulation in human breast cancer. *Cancer Res* **65**:7065–7070.
18. Jiang MC, Luo SF, Li LT, Lin CC, Du SY, Lin CY *et al* (2007) Synergic CSE1L/CAS, TNFR-1, and p53 apoptotic pathways in combined interferon-gamma/adriamycin-induced apoptosis of Hep G2 hepatoma cells. *J Exp Clin Cancer Res* **26**:91–99.
19. Kefas B, Godlewski J, Comeau L, Li Y, Abounader R, Hawkinson M *et al* (2008) microRNA-7 inhibits the epidermal growth factor receptor and the Akt pathway and is down-regulated in glioblastoma. *Cancer Res* **68**:3566–3572.
20. Kozaki K, Imoto I, Mogi S, Omura K, Inazawa J (2008) Exploration of tumor-suppressive microRNAs silenced by DNA hypermethylation in oral cancer. *Cancer Res* **68**:2094–2105.
21. Kutay U, Bischoff FR, Kostka S, Kraft R, Görlich D (1997) Export of importin alpha from the nucleus is mediated by a specific nuclear transport factor. *Cell* **90**:1061–1071.
22. Lagos-Quintana M, Rauhut R, Lendeckel W, Tuschl T (2001) Identification of novel genes coding for small expressed RNAs. *Science* **294**:853–858.
23. Lagos-Quintana M, Rauhut R, Yalcin A, Meyer J, Lendeckel W, Tuschl T (2002) Identification of tissue-specific microRNAs from mouse. *Curr Biol* **12**:735–739.
24. Langevin SM, Stone RA, Bunker CH, Lyons-Weiler MA, LaFramboise WA, Kelly L *et al* (2011) MicroRNA-137 promoter methylation is associated with poorer overall survival in patients with squamous cell carcinoma of the head and neck. *Cancer* **117**:1454–1462.
25. Li KK, Pang JC, Ching AK, Wong CK, Kong X, Wang Y *et al* (2009) miR-124 is frequently down-regulated in medulloblastoma and is a negative regulator of SLC16A1. *Hum Pathol* **40**: 1234–1243.
26. Liang Y, Ridzon D, Wong L, Chen C (2007) Characterization of microRNA expression profiles in normal human tissues. *BMC Genomics* **8**:166. doi:10.1186/1471-2164-8-166.
27. Lo SS, Hung PS, Chen JH, Tu HF, Fang WL, Chen CY *et al* (2012) Overexpression of miR-370 and downregulation of its novel target TGFβ-RII contribute to the progression of gastric carcinoma. *Oncogene* **31**:226–237.
28. Lorenzato A, Martino C, Dani N, Oligschläger Y, Ferrero AM, Biglia N *et al* (2012) The cellular apoptosis susceptibility CAS/CSE1L gene protects ovarian cancer cells from death by suppressing RASSF1C. *FASEB J* **26**:2446–2456. doi:10.1096/fj.11-195982.
29. Louis DN, Ohgaki H, Wiestler OD, Cavenee WK (eds) (2007) *In: WHO Classification of Tumours of the Central Nervous System*, 4th edn. IARC Press: Lyon, France.
30. Medina PP, Slack FJ (2008) microRNAs and cancer: an overview. *Cell Cycle* **7**:2485–2492.
31. Meng F, Henson R, Wehbe-Janek H, Ghoshal K, Jacob ST, Patel T (2007) MicroRNA-21 regulates expression of the PTEN tumor suppressor gene in human hepatocellular cancer. *Gastroenterology* **133**:647–658.
32. O'Donnell KA, Wentzel EA, Zeller KI, Dang CV, Mendell JT (2005) c-Myc-regulated microRNAs modulate E2F1 expression. *Nature* **435**:839–843.
33. Peiró G, Diebold J, Löhrs U (2002) CAS (cellular apoptosis susceptibility) gene expression in ovarian carcinoma: correlation with 20q13.2 copy number and cyclin D1, p53, and Rb protein expression. *Am J Clin Pathol* **118**:922–929.
34. Seiden-Long IM, Brown KR, Shih W, Wigle DA, Radulovich N, Jurisica I, Tsao MS (2006) Transcriptional targets of hepatocyte growth factor signaling and Ki-ras oncogene activation in colorectal cancer. *Oncogene* **25**:91–102.
35. Sempere LF, Freemantle S, Pitha-Rowe I, Moss E, Dmitrovsky E, Ambros V (2004) Expression profiling of mammalian microRNAs uncovers a subset of brain-expressed microRNAs with possible roles in murine and human neuronal differentiation. *Genome Biol* **5**:R13.
36. Silber J, Lim DA, Petritsch C, Persson AI, Maunakea AK, Yu M *et al* (2008) miR-124 and miR-137 inhibit proliferation of glioblastoma multiforme cells and induce differentiation of brain tumor stem cells. *BMC Med* **6**:14. doi:10.1186/1741-7015-6-14.
37. Skalsky RL, Cullen BR (2011) Reduced expression of brain-enriched microRNAs in glioblastomas permits targeted regulation of a cell death gene. *PLoS ONE* **6**:e24248.
38. Smrt RD, Szulwach KE, Pfeiffer RL, Li X, Guo W, Pathania M *et al* (2010) MicroRNA miR-137 regulates neuronal maturation by targeting ubiquitin ligase mind bomb-1. *Stem Cells* **28**:1060–1070.
39. Spahn M, Kneitz S, Scholz CJ, Stenger N, Rüdiger T, Ströbel P *et al* (2010) Expression of microRNA-221 is progressively reduced in aggressive prostate cancer and metastasis and predicts clinical recurrence. *Int J Cancer* **127**:394–403.
40. Tai CJ, Shen SC, Lee WR, Liao CF, Deng WP, Chiou HY *et al* (2010) Increased cellular apoptosis susceptibility (CSE1L/CAS) protein expression promotes protrusion extension and enhances migration of MCF-7 breast cancer cells. *Exp Cell Res* **316**:2969–2981.
41. Tanaka T, Ohkubo S, Tatsuno I, Prives C (2007) hCAS/CSE1L associates with chromatin and regulates expression of select p53 target genes. *Cell* **130**:638–650.
42. Wiklund ED, Gao S, Hulf T, Sibbritt T, Nair S, Costea DE *et al* (2011) MicroRNA alterations and associated aberrant DNA methylation patterns across multiple sample types in oral squamous cell carcinoma. *PLoS ONE* **6**:e27840.
43. Xia H, Cheung WK, Ng SS, Jiang X, Jiang S, Sze J *et al* (2012) Loss of brain-enriched miR-124 MicroRNA enhances stem-like

traits and invasiveness of glioma cells. *J Biol Chem* **287**: 9962–9971.
44. Zhang Y, Chao T, Li R, Liu W, Chen Y, Yan X *et al* (2009) MicroRNA-128 inhibits glioma cells proliferation by targeting transcription factor E2F3a. *J Mol Med (Berl)* **87**:43–51.
45. Zhu S, Wu H, Wu F, Nie D, Sheng S, Mo YY (2008) MicroRNA-21 targets tumor suppressor genes in invasion and metastasis. *Cell Res* **18**:350–359.

SUPPORTING INFORMATION

Additional Supporting Information may be found in the online version of this article:

Figure S1. Kaplan–Meier (left) OS and (right) PFS estimates on (A and D) age, (B and E) grade, and (C and F) oligoastrocytic phenotype in 25 oligodendroglial tumors.

Figure S2. Kaplan-Meier survival analysis for (A) OS and (B) PFS in Grade II patients. Patients with <median of miR-137 expression showed shorter PFS than patients with ≥median of miR-137 expression.

Figure S3. Luciferase reporter assay on AKT, CDC 42, and NRP1. Four luciferase reporter plasmids were prepared. They contained putative binding sites of miR-137 on 3'UTRs of AKT, CDC42, and NRP1. Cotransfection of firefly luciferase reporter plasmid, pRL-TK Renilla plasmid (for normalization), and miR-137 or negative control were achieved in LNZ308 cells.

Figure S4. Effectiveness of CSE1L-specific siRNAs. TC620, U87, and U373 cells were transfected with two siRNAs against CSE1L or a negative control. Expression of CSE1L was determined by Western blot analysis at 24 and 48 h post-transfection. GAPDH was served as an internal control.

Table S1. Clinicopathological information of 35 oligodendroglial tumors studied.